Al-Tous, Hanan; Tirkkonen, Olav; Liang, Jing

Adaptive Sector Splitting based on Channel Charting in Massive MIMO Cellular Systems

Published in:
Proceedings of IEEE 93rd Vehicular Technology Conference, VTC 2021

DOI:
10.1109/VTC2021-Spring51267.2021.9448830

Published: 15/06/2021

Document Version
Peer-reviewed accepted author manuscript, also known as Final accepted manuscript or Post-print

Please cite the original version:
Al-Tous, H., Tirkkonen, O., & Liang, J. (2021). Adaptive Sector Splitting based on Channel Charting in Massive MIMO Cellular Systems. In *Proceedings of IEEE 93rd Vehicular Technology Conference, VTC 2021* Article 9448830 (IEEE Vehicular Technology Conference). IEEE. https://doi.org/10.1109/VTC2021-Spring51267.2021.9448830

Adaptive Sector Splitting based on Channel Charting in Massive MIMO Cellular Systems

Hanan Al-Tous*, Olav Tirkkonen* and Jing Liang†

*Department of Communications and Networking, Aalto University, Espoo, Finland
†Huawei Technologies CO., LTD., Shanghai Institute No. 2222, Xinjinqiao Road, Pudong, Shanghai, 201206, P.R. China
Email:{hanan.al-tous, olav.tirkkonen}@aalto.fi, jingliang@huawei.com

***Abstract*—We consider a downlink scenario where a multiantenna base station in a sectorized cellular system creates multiple logical cells in each sector, applying Adaptive Sector Splitting (ASS). In ASS, a population of User Equipments (UEs) is grouped based on radio Channel State Information (CSI), groups are assigned to cells, and the virtual antennas serving the cells are optimized based on CSI. Grouping UEs based on covariance matrix similarity may result in considerable spatial overlap of the UE groups, and a need for frequent handovers for mobile UEs. To reduce handovers, an improved grouping strategy that takes into account UE physical locations is needed. We use Channel Charting (CC) to learn the radio map of the cell from uplink CSI, and consider UE grouping based on CC locations aiming to maximize the mean distance of UEs to virtual cell borders without the need to know the physical locations of the UEs. Simulation results show that ASS groups based on CC are more compact than angle-of-arrival and covariance matrix based groupings from the literature.**

***Index Terms*—Adaptive sector splitting, UE clustering, precoding, channel charting.**

I. Introduction

5G New Radio (5GNR) is a beam-oriented cellular system, where the network can flexibly configure what beams are used by Base Stations (BSs), and which beams a User Equipment (UE) is aware of [1], [2]. This flexibility is an important component in future proofing 5GNR towards increasing number of antennas, to harvest massive MIMO gains [3] and extending coverage to higher frequency ranges [4]. Furthermore, to reduce complexity, individual antenna elements are not accessible from transmitter baseband—hybrid precoding systems [5] are applied. As a consequence, beam management is an important component of 5G and Beyond Fifth-Generation (B5G) systems.

A 5GNR Base Station (BS) creates a number of beams, possibly using analog beamforming technologies, and sends Channel State Information (CSI) Reference Signals on them. A UE is configured to measure and report CSI from up to four downlink beams [1]. If a UE has multiple antennas, and a beamforming capability, selection of the best UE beam is assumed in the process of CSI reporting. For a mobile UE, efficient control of handovers between beam boundaries is important to have a stable service. To reduce the management burden of beam handovers, virtual cells consisting of a collection of beams can be created and the concept of beam handover can be replaced with a concept of handover between virtual cells. While such a mechanism would be an optional optimization for 5GNR and B45G systems, it would be a necessity in backward compatible operation, where UEs may comply to LTE-A or LTE specifications, where UEs can recognize only eight or four BS transmission antennas [6], [7].

In Adaptive Sector Splitting (ASS) a multiantenna BS divides its transmission into several virtual cells, each cell consisting of a number of virtual antennas. To comply with with both 5GNR [1] and LTE [6] UE reporting principles, we assume that a virtual cell consists of four virtual antennas.

In [8], the authors considered a k-means clustering algorithm to partition users into groups with sufficiently similar channel covariance eigenspaces. A greedy sum-rate maximization scheduling algorithm for users in the groups. Different similarity measures for user clustering based on weighted likelihood, subspace projections and the Fubini-Study metric were considered in [9], along with different clustering methods, including hierarchical and k-medoids clustering. In [10], the authors developed a new clustering and scheduling algorithm based on graph theory that outperformed other clustering and scheduling schemes in both sum-rate and throughput fairness.

It can be observed that all prior art studies, performance of a clustering algorithm was evaluated in terms of the sum rate or rate fairness. However, UEs within the same group based on channel covariance statistics may not be located in nearby physical locations. This means that group assignment may need to be changed frequently for mobile UEs. which can equivalently be considered as a handover event between group-specific cells. To reduce the burden on the network from handovers, we introduce a statistic to measure the compactness of UE groups; handover distance is measured as the distance of a UE to the nearest border between virtual cells. Grouping of mobile UEs then becomes a tradeoff between spectral efficiency and handover distance. Clustering of UEs based on physical location information would lead to perfect control of handover distance. However, UE location information is generically not available at BSs.

A novel Channel Charting (CC) framework is proposed for massive MIMO systems in [11], exploiting the massive amounts of Channel State Information (CSI) available at the BSs. In CC, unsupervised machine learning techniques are

This work was funded in part by Huawei Technologies Co., Ltd.

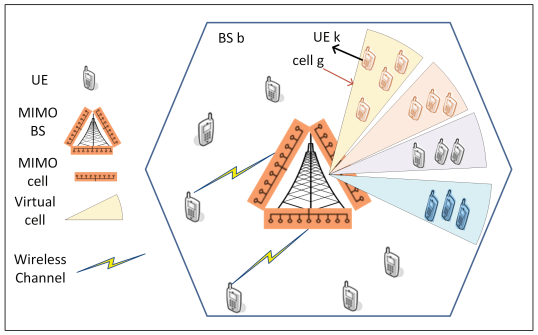

Fig. 1: System model: a MIMO cellular BS, consists of 3 cells, each cell is divided into 4 virtual cells.

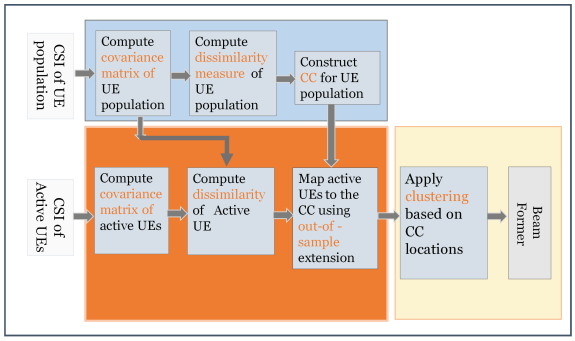

Fig. 2: ASS operation based on CC. The main CC steps are shown in three background blocks. Off-line construction of a CC is in the upper part. Steps for out-of-sample CC for an active user are low-left, and CC based grouping and beamforming steps are low-right.

used to create a radio map of the cell, which preserves the neighborhood relations of UEs.

In this paper, we analyze the tradeoff between spectral efficiency and handover distance. To have compact UE groups, leading to a reduced number of handover events, we use vicinity in a CC as a proxy of spatial vicinity of UEs, and cluster UEs based on CC locations.

The remainder of this paper is organized as follows. In Section II, the system model is presented. In Section III, CC basic concepts are introduced. In Section IV, ASS we discuss CC-based grouping principles. Simulation settings and numerical results are presented and discussed in Section V. Finally, conclusions are drawn in Section VI.

II. System Model

We consider a massive MIMO cellular system consisting of B BSs, where the BS operate in a sectorized manner, serving three sectors. There is a Uniform Planar Array (UPA) with M' antennas serving each sector. The total number of antennas at the BS $M = 3M'$. For simplicity, we assume that each UE has one omnidirectional antenna, handling more involved UE antenna configurations of 5GNR is left for future work. The system model for BS b is shown in Figure 1.

In each sector, there is a downlink multiuser MIMO system, where the cell splits the set of active UEs into G virtual cells. In virtual cell g there are M_g virtual antennas. The UEs belonging to the same virtual cell are called a group or a cluster. The maximum number of UEs that can be served simultaneously in a virtual cell is M_g. If the number of active UEs in a virtual cell is larger than M_g, a scheduling algorithm such as round robin can be considered. For concrete results, we consider $G = 4$, $M_g = 4$ for all g, and $M' = 32$.

A. Precoder in Sector

The downlink beamformer is implemented in two stages in the form $\mathbf{W} = \mathbf{BV}$, as in [12]. The outer beamformer $\mathbf{B}$ separates the UE groups belonging to the virtual cells, and is designed to maximize a lower bound of the average Signal to-Leakage-Noise-Ratio (SLNR). The inner beamformer $\mathbf{V}$ separates users within the group. It is implemented using the Zero-Forcing (ZF) principle to cancel the interference from simultaneously served UEs in the virtual cell.

The outer beamformer is partitioned into G sub-matrices as $\mathbf{B} = [\mathbf{B}_1, \ldots, \mathbf{B}_G]$, with $\mathbf{B}_g = [\mathbf{b}_{g,1}, \ldots, \mathbf{b}_{g,M_g}] \in \mathbb{C}^{M' \times M_g}$, satisfying $\mathbf{B}_g^H \mathbf{B}_g = \mathbf{I}_{M_g}$, where $\mathbf{I}_n$ is the identity matrix of dimension n. The dimension of effective channel seen by the inner beamformer is M_g. The inner beamformer $\mathbf{V}$ has a block diagonal structure in the group dimension; $\mathbf{V} = \mathrm{diag}(\mathbf{V}_1, \mathbf{V}_2, \ldots, \mathbf{V}_G)$, with $\mathbf{V}_g = [\mathbf{v}_{g,1}, \mathbf{v}_{g,2}, \ldots, \mathbf{v}_{g,S_g}] \in \mathbb{C}^{M_g \times S_g}$ and S_g is the number of data streams for group g. Here, we assume that one data stream is transmitted for each UE in the group, i.e., $S_g = M_g$. The outer beamformer for each virtual cell is designed by solving the Trace-Quotient-Problem (TQP) based on the channel statistics. The inner precoder of each virtual cell is implemented using ZF principle based on the instantaneous effective channel realizations [12].

B. ASS Operation

We are interested in reducing the number of handover events between virtual cells for mobile UEs in the sector. In the literature [8], [10] UEs clustering has been based on grouping UEs that either have identical covariance or similar covariance matrices. The downside of such grouping is that the cost of handover is not taken into consideration for mobile UEs. Motivated by this, we consider a new grouping approach based on CC. Active UEs are divided into G virtual cells in which neighboring UEs as determined by the CC are grouped into the same cluster (virtual cell).

The block diagram of CC-based ASS is shown in Figure 2. First, in a training phase, a CC is constructed for a large set of UEs based on long-term uplink channel covariance CSI measured at the BS or at multiple BSs. A dimensionality reduction technique is then applied to construct the relative location chart. At run-time, active UEs in the cell are located to the channel chart based on CSI measured at the BS. An out-of-sample CC algorithm [13] can be used for this. Based on the CC locations, active UEs are then grouped into G virtual groups using a clustering algorithm such as the k-means algorithm.

III. Basics of Channel Charting

CC is based on the assumption that statistical properties of MIMO channels vary relatively slowly across space, on

a length-scale related to the macroscopic distances between scatterers in the channel, not on the small fading length-scale of wavelengths [11], [14]. In addition, it is assumed that there is a continuous mapping from the spatial location $\boldsymbol{y}_k$ of UE k to the BS long-term CSI covariance matrix $\boldsymbol{R}_{k,b}$;

$$\mathcal{H}_b : \mathbb{R}^d \to \mathbb{C}^{M\times M}; \quad \mathcal{H}_b(\boldsymbol{y}_k) = \boldsymbol{R}_{k,b}. \tag{1}$$

Here $d = 2$ or 3 is the spatial dimension and M is the number of antennas at the BS. In this regard, the long-term CSI covariance matrix can be used to capture large-scale effects of the wireless channel, and provides location information.

CC starts by extracting suitable channel features from the long-term CSI covariance matrix $\boldsymbol{R}_{k,b}$, which capture large-scale properties of the wireless channel. CC then proceeds by using the set of features collected for the set of UEs $\mathcal{K}_b = \{1, \ldots, K_b\}$ seen by BS b to learn a dissimilarity matrix $\boldsymbol{D}_b \in \mathbb{R}_+^{K_b\times K_b}$. The pairwise dissimilarity $[\boldsymbol{D}_b]_{k,k'}$ between UEs $k, k' \in \mathcal{K}_b$ measures the dissimilarity of the radio features between these UEs. Different criteria can be used to select the channel features and for computing the dissimilarity matrix see [11], [14]. In this paper, we consider the CSI covariance matrices as features and construct the dissimilarity matrix based on the Collinearity Matrix Distance (CMD). The CMD between UE k and UE k' at BS b is computed as [15]:

$$d_{CMD}\big(\boldsymbol{R}_{k,b}, \boldsymbol{R}_{k',b}\big) = 1 - \frac{|\mathrm{Tr}(\boldsymbol{R}_{k,b}\boldsymbol{R}_{k',b})|}{||\boldsymbol{R}_{k,b}||_F||\boldsymbol{R}_{k',b}||_F}, \tag{2}$$

where $\mathrm{Tr}(\mathbf{A})$ denotes the trace of matrix $\mathbf{A}$ and $||\mathbf{A}||_{\mathbf{F}}$ denotes the Frobenius norm of matrix $\mathbf{A}$.

Next a low dimensional channel chart is found in an self-supervised manner, providing chart locations $\{\boldsymbol{z}_k\}_{k=1}^{K_b}$ for the set of UEs $\mathcal{K}_b$ such that UEs that are neighbors in the ground truth physical space will be neighbors in the channel chart. A channel chart is constructed using an unsupervised machine learning framework based on manifold learning. The aim is to preserve as much of the significant structure of the high-dimensional data as possible in the low-dimensional chart.

Here, we use Laplacian Eigenmaps (LE) and t-Distributed-Stochastic-Neighbor-Embedding (t-SNE) dimensionality reduction techniques [16], [17]. LE and t-SNE are good candidates for dimensionality reduction in CC, as shown in [14]. The performance of the CC can be evaluated using the Continuity (CT) and Trustworthiness (TW) measures, related to neighborhood preservation, and Kruskal's Stress (KS), related to preserving global geometry, see [18], [19].

Multipoint Channel Charting (MPCC) is a distributed algorithm, extending Single-Point CC (SPCC) to multiple BSs. CSI features and dissimilarity matrices are computed at each BS and then merged into a global dissimilarity matrix using a fusion center [14]. MPCC utilizes the different views of the spatially distributed BSs by fusing the BS-specific dissimilarity matrices $\boldsymbol{D}_b,\ b = 1, \ldots, B$ into a global dissimilarity matrix $\boldsymbol{D} \in \mathbb{R}_+^{K\times K}$ for K UEs.

It is important to accurately estimate the CC location of active UEs without repeating the CC procedure again. Extension-of-MPCC/CC to out-of-sample data points based on LE is considered in [13]. The t-SNE algorithm with a parametric implementation can also be used for out of sample data, the mapping can be parameterized by means of a deep neural network, for details see [17].

IV. ASS Grouping Algorithms

A clustering algorithm can be implemented either on a population level or on the level of an active set. Population level clustering is a static approach based on the radio characteristics of the whole population (i.e., covariance matrices, AoAs, physical location, CC location). Clustering is implemented once in training phase, and at run-time each active UE is assigned to its nearest characteristic cluster. The problem with this approach is that at run-time, we do not have control on the number of UEs in each group. In an extreme case, all active UEs could be in one group. To avoid this problem, we consider grouping of the active set of users, irrespectively of the grouping principle applied.

A. Grouping Principles from the Literature

We consider two clustering methods from the literature; direct covariance matrix based grouping [8] and Angle-of-Arrival (AoA) based grouping [20]. For direct covariance matrix based clustering [8], the chordal distance is used to measure the distance between long-term covariance matrices. Clustering based on similar covariance matrices maximizes the sum rate as shown in [8], [12], [21]. The k-means clustering algorithm is used, based on Lloyd's algorithm [22]. AoA clustering [20] is based on finding the dominant beam AoA of each UE long-term covariance matrix, using the Multiple-Signal-Classification (MUSIC) algorithm [23], then performing 1D k-means clustering using the AoAs.

Furthermore, we consider grouping of UEs based on the 2D physical locations using the k-means algorithm, assuming that UEs physical locations are known to the BSs.

B. CC Based Grouping Principle

To create the CC and preserve the neighborhoods of UEs, a large data set of covariance CSI from UEs at different locations is needed. It is not sufficient to just use CSI of an active set of UEs to create a CC. For CC-based grouping, we consider a sample of A_c active UEs, then based on out-of-sample CC locations, the active UEs are place on the CC, and then clustered into G groups using the k-means algorithm based on *SPCC/MPCC locations*.

C. User Grouping Quality Measures

To investigate the effect of the overlap of clusters on handover, we consider the minimum distance between UE k in group g and all UEs in other groups:

$$d_k^{\min} = \min_{m\notin g} d_{k,m}, \text{ for } k \in g, \tag{3}$$

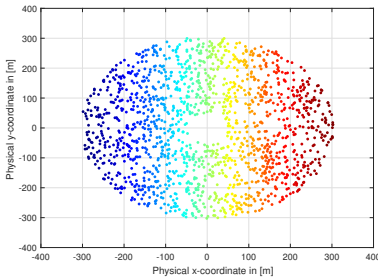

Fig. 3: UE physical locations for CC. Sampled UE locations marked by colors.

where $d_{k,m} = ||\mathbf{y}_k - \mathbf{y}_m||_2$ is the Euclidean distance between the 2D physical ground truth locations of UE k and UE m. The handover distance d_{Ho} of an active set of A_c UEs is then:

$$d_{\text{Ho}} = \frac{1}{A_c} \sum_{k=1}^{A_c} d_k^{\min}. \tag{4}$$

The *average handover distance* over realizations measures the performance of a clustering algorithm with respect to the amount of group overlap, and the related rate of handovers.

The probability of a small handover distance of $d_k^{\min} \leq$ 30m is a complementary measure of clustering quality. It is related to the probability that a vehicular user moving at a speed of 50 km/h faces a handover within the time of 1 s, assuming that group boundary is half-way between the closest users belonging to different groups. Note that the handover distance is characterizing the *average* distance of active users to neighboring virtual cells.

D. Spectrum Efficiency

For different grouping algorithms, the spectral efficiency is evaluated by considering Multiple Access Interference (MAI) from transmissions to users in different groups in the same sector, as well as co-channel inference from different sectors and BSs, as well thermal noise. The performance of different grouping algorithms is evaluated in terms of the average spectrum efficiency and the 5% UE spectral efficiency.

V. Simulations

A. Simulation Settings

We use the Quasi-Deterministic-Radio-Channel-Generator (Quadriga) [24] to simulate the radio environment and to obtain the CSIs of the wireless channels. The environment parameters follow the 3GPP 38.901 UMa-NLOS scenario [25]. We consider a hexagonal network layout of 7 BSs, each with three sectors. The Inter Site Distance between BSs is 500 m. The BS height is 25 m, and the ratio of indoor users is 0.8. The 3GPP antenna model [25] is used in each sector with $M' = 32$ antennas, with two cross-polarized antennas arranged in 8 horizontal and two vertical positions with half wavelength horizontal and vertical spacing, and a downtilt angle of 7°. An omnidirectional antenna is used at each UE. The carrier frequency is 1.84 GHz, the bandwidth is 10 MHz, and there are 512 subcarriers. The cell transmit power is 49 dBm. Thermal noise power spectral density at the UEs is -174 dBm/Hz, and the UE noise figure is 9 dB.

Channels are generated based on 10 clusters of multi-path components, and 20 sub-paths in each cluster. To reduce run-time and memory requirements, precise CSI from 4 nearest BSs are only generated for each UE, with interference from other BSs modeled only based on path loss. To estimate the long-term covariance matrix at the BSs, 15 spatial/time samples in a spatial distance of 1 m are considered, where each UE is assumed to move in a straight line with a random direction.

To create a CC, 1500 UEs are uniformly distributed in an annuls of inner radius of 50 m and outer radius of 300 m. For run-time evaluation of ASS performance, we consider 1000 UE drops with 30 active UEs dropped in the sector of interest. Multiple Access Control is modeled by assuming round robin scheduling over 100 subframes. In each subframe $M_g = 4$ UEs are served in each group, in total 16 UEs are served in each subframe in the sector of interest.

B. Inference Modeling

We consider the inference from downlink transmission of other cells, sectors and BSs in the layout. The interference power is computed from three classes: 1) MAI within a sector is modeled assuming perfect CSI at the BS of the in-group fast fading channels. The outer beamformers are designed to maximize the SLNR using the TQP algorithm [12]. Interference from transmissions to UEs in the same group is cancelled by ZF. MAI arises from the lack of CSI between groups. 2) co-channel interference from 3 neighboring BSs (each with 3 sectors) and the other 2 sectors from the serving BS is computed by using the instantaneous CSIs and random beamformers, i.e., 16 random beams in each interfering sector. 3) interference from the remaining BSs in the network layout is computed modeled by the average interference arising from the 3GPP 38.900 UMa path loss model.

C. Results and Discussion

The physical locations of the UEs used in the CC creation phase is shown in Figure 3, and the SPCC and MPCC results are shown in Figure 4. To construct a MPCC, each UE is assumed to be seen by 4 BSs, and the dissimilarity matrices of 7 BSs are merged as in [14]. The CT and TW performance measures are in the range 0.84-0.86 and the KS is 0.38-0.40.

Numerical results for the clustering metrics can be found in Table I, where both mean and 5% spectral efficiency, as well as mean handover distance d_{Ho} and the probability of small handover distance $d_{\text{Ho}} <$ 30m are tabulated.

The *SPCC t-SNE* based grouping achieves both the largest mean and 5% spectral efficiency of the CC-based grouping methods. The sum spectral efficiency of the *best CC based grouping is comparable with the sum spectral efficiency of AoA based grouping*, and slightly worse with 5% spectral efficiency. Covariance matrix based grouping achieves the largest spectral efficiency, as expected. If CC would accurately

TABLE I: Spectral Efficiency and Handover Distance for Different Grouping Algorithms

Performance	Channel Charting				Non-Channel Charting			
	SPCC LE	MPCC LE	SPCC t-SNE	MPCC t-SNE	Physical	Covariance	AoA	Random
Sum Spectral Efficiency in [bits/Hz]	7.70	5.80	8.18	4.91	9.77	11.69	8.67	5.04
5% UE Spectral Efficiency in [bits/Hz]	0.038	0.034	0.044	0.016	0.038	0.067	0.053	0.016
Mean Handover Distance in [m]	60.1	70.8	51.2	53.6	74.8	53.6	48.5	40.6
Probability of Handover Distance < 30 m	0.22	0.05	0.23	0.13	0.10	0.21	0.23	0.45

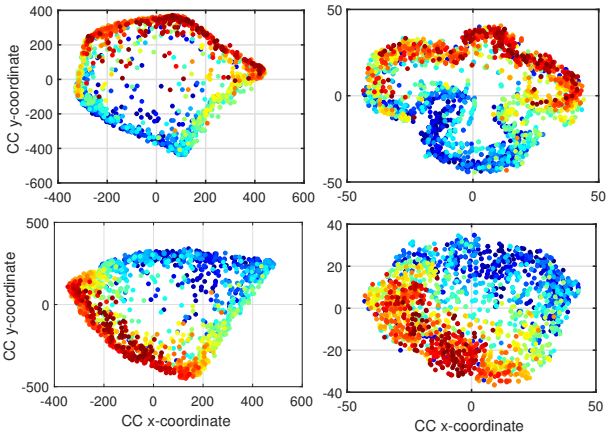

Fig. 4: (Top-Left); SPCC LE based. (Top-Right); SPCC t-SNE based. (Bottom-Left); MPCC LE based. (Bottom-Right) MPCC t-SNE based. CC locations marked by colors corresponding to the ground truth locations of Figure 3.

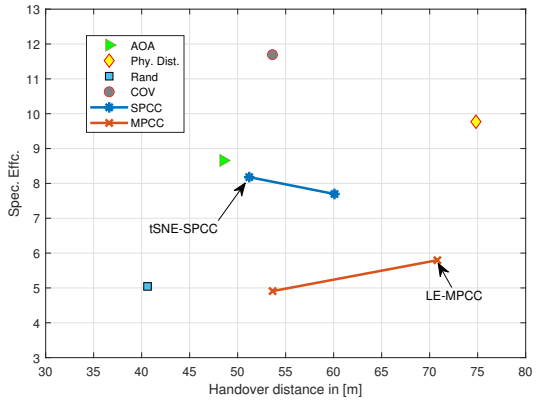

Fig. 5: Tradeoff of spectral efficiency versus Handover distance for different grouping algorithms.

recover the physical locations, we would expect CC to achieve the performance of physical location based grouping.

When it comes to the handover distance, *MPCC LE* based grouping outperforms CC based groupings, and CC-based grouping algorithms generically outperform covariance matrix and AoA based grouping with significant margins. Physical location based grouping achieves the largest mean handover distance, but *MPCC LE* approaches its performance, and interestingly provides a *lower* probability for small handover distance. This is indicating that simply using the k-means algorithm may not be sufficient if we want to control the compactness of UE clusters for ASS. Clustering algorithms taking the handover distance may be needed.

Our objective is to trade off spectral efficiency against handover, and we have two spectral efficiency metrics and two handover metrics, and thus four versions of the tradeoff. Two of these are investigated in more detail. The sum spectral efficiency vs. mean d_{Ho} tradeoff is depicted in Figure 5, and the sum spectral efficency vs. probability of small d_{Ho} in Figure 6. When trading off two variables, an algorithm is strictly better than another if it is at least as good for one variable, and better in the other.

When comparing the different CC-algorithms, the results are inconclusive. The MPCC algorithm based on t-SNE is strictly outperformed by some other CC algorithm for any combination of a spectral efficiency and a handover performance measures. The three other algorithms lie on the tradeoff-curves for CC-based grouping.

In the sum spectral efficiency vs. mean d_{Ho} tradeoff, the best realizable schemes are the covariance based, *LE-SPCC* and *LE-MPCC* algorithms. The spectral efficiency reduces and d_{Ho} increases in this order. In the sum spectral efficiency vs. probability of small d_{Ho} tradeoff, the best realizable schemes are the covariance based *LE-MPCC* algorithms. The spectral efficiency reduces and the probability of small d_{Ho} decreases in this order. It is particularly interesting that from perspective of both of these tradeoffs, the AoA-based algorithm is strictly outperformed by the covariance based clustering algorithm. The CC-based algorithms are capable of improving on the handover metrics of the covariance matrix algorithm; approaching, and sometimes even outperforming, the hypothetical algorithm based on ground truth physical location information. The cost in spectral efficiency is considerable, however.

VI. Conclusion

In this paper we considered a CC based UE grouping approach for adaptive sector splitting in a cellular system. First, a channel chart is constructed, based on a data set of uplink CSI measurement. At run-time, given a set of active users in a sector of a base station, a k-means clustering algorithm is used to cluster active UEs based on their CC locations. Virtual cells are constructed in the sector to serve these user groups. We considered round robin time domain scheduling for UEs in the same group and used two-stage hierarchical precoder; the outer precoder maximizes a lower

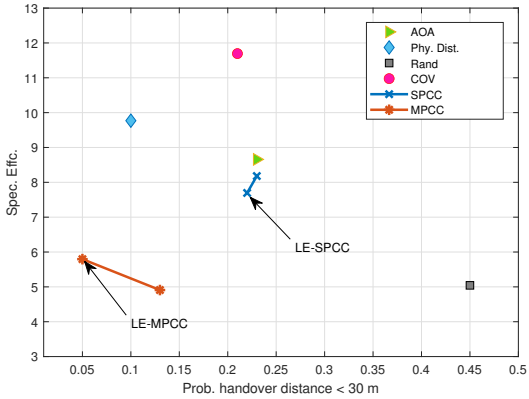

Fig. 6: Tradeoff of spectral efficiency versus Probability of handover distance being less than 30 m for different grouping algorithms.

bound of the average SLNR based on large scale CSIs of active UEs, whereas the inner precoder is based on the instantaneous CSI of the effective channels of the scheduled UEs and using a ZF principle to cancel intra group interference.

We simulated the radio environment using the QuaDRiGa wireless channel simulator and evaluated the performance of the ASS for different grouping algorithms, investigating the tradeoff between system spectral efficiency and expected distance to next handover event for mobile UEs. Our simulation results showed that CC provides comparable spectral efficiency to an AoA-based algorithm, and larger mean handover distance. Covariance matrix based grouping provides best spectral efficiency, with a compromised handover distance. The mean handover distance of the best MPCC scheme approaches the performance of ground truth physical location based grouping.

In future work, we shall improve the grouping algorithms in two directions. First, we shall develop CC based grouping with controlled group sizes to assign similar number of UEs to each group. Second, we shall incorporate handover distance directly into the grouping metric. Different CSI features and dissimilarity measures are going to be designed to improve the CC performance. In addition, we shall expand the modeling to cover multiantenna UEs with autonomous UE Rx-beam management.

REFERENCES

[1] 3GPP, "NR; Physical layer measurements," 3rd Generation Partnership Project (3GPP), Technical Specification TS 38.215, Jan. 2018, version 15.0.0.

[2] M. Giordani, M. Polese, A. Roy, D. Castor, and M. Zorzi, "A tutorial on beam management for 3GPP NR at mmWave frequencies," *IEEE Commun. Surveys Tuts.*, vol. 21, no. 1, pp. 173–196, 2019.

[3] T. L. Marzetta, "Noncooperative cellular wireless with unlimited numbers of base station antennas," *IEEE Trans. Wireless Commun.*, vol. 9, no. 11, pp. 3590–3600, 2010.

[4] S. A. Busari, K. M. S. Huq, S. Mumtaz, L. Dai, and J. Rodriguez, "Millimeter-wave massive MIMO communication for future wireless systems: A survey," *IEEE Commun. Surveys Tuts.*, vol. 20, no. 2, pp. 836–869, Second quarter 2018.

[5] X. Gao, L. Dai, S. Han, C. I, and R. W. Heath, "Energy-efficient hybrid analog and digital precoding for mmWave MIMO systems with large antenna arrays," *IEEE Journal on Selected Areas in Communications*, vol. 34, no. 4, pp. 998–1009, 2016.

[6] 3GPP, "Physical channels and modulation," 3rd Generation Partnership Project (3GPP), Evolved Universal Terrestrial Radio Access (E-UTRA) 36.211, feb. 2013, version 11.2.0.

[7] ——, "Study on elevation beamforming/full-dimension (FD) MIMO for LTE," 3rd Generation Partnership Project (3GPP), technical document number 36.897, nov. 2014, version 12.

[8] J. Nam, A. Adhikary, J. Ahn, and G. Caire, "Joint spatial division and multiplexing: Opportunistic beamforming, user grouping and simplified downlink scheduling," *IEEE J. Sel. Topics Signal Process.*, vol. 8, no. 5, pp. 876–890, Oct. 2014.

[9] Y. Xu, G. Yue, and S. Mao, "User grouping for massive MIMO in FDD systems: New design methods and analysis," *IEEE Access*, vol. 2, pp. 947–959, 2014.

[10] A. Maatouk, S. E. Hajri, M. Assaad, and H. Sari, "On optimal scheduling for joint spatial division and multiplexing approach in FDD massive MIMO," *IEEE Trans. Signal Process.*, vol. 67, no. 4, pp. 1006–1021, 2019.

[11] C. Studer, S. Medjkouh, E. Gönültaş, T. Goldstein, and O. Tirkkonen, "Channel charting: Locating users within the radio environment using channel state information," *IEEE Access*, vol. 6, pp. 47 682–47 698, 2018.

[12] D. Kim, G. Lee, and Y. Sung, "Two-stage beamformer design for massive MIMO downlink by trace quotient formulation," *IEEE Trans. Wireless Commun.*, vol. 63, no. 6, pp. 2200–2211, Jun. 2015.

[13] T. Ponnada, H. Al-Tous, O. Tirkkonen, and C. Studer, "An out-of-sample extension for wireless multipoint channel charting," in *Proc. of 14th EAI International Conference on Cognitive Radio Oriented Wireless Networks,(Crowncom)*, Jun. 2019.

[14] J. Deng, S. Medjkouh, N. Malm, O. Tirkkonen, and C. Studer, "Multipoint channel charting for wireless networks," in *Proc. of 52nd Asilomar Conference on Signals, Systems, and Computers*, Oct. 2018, pp. 286–290.

[15] M. Kurras, S. Dai, S. Jaeckel, and L. Thiele, "Evaluation of the spatial consistency feature in the 3GPP geometry-based stochastic channel model," in *Proc. of IEEE Wireless Communications and Networking Conference (WCNC)*, Apr. 2019, pp. 1–6.

[16] L. Maaten, E. Postma, and H. Herik, "Dimensionality reduction: A comparative review," 2008.

[17] L. van der Maaten, "Learning a parametric embedding by preserving local structure," in *AISTATS*, 2009.

[18] J. Venna and S. Kaski, "Neighborhood preservation in nonlinear projection methods: An experimental study," in *Proc. of the International Conference on Artificial Neural Networks, (ICANN)*, 2001, pp. 485–491.

[19] A. G. Berna, S. Gonzalez, V. Robles, and E. M. Ruiz, "A methodology to compare dimensionality reduction algorithms in terms of loss of quality," *Inf. Sci.*, vol. 270, pp. 1–27, 2014.

[20] X. Zhang, J. Tadrous, E. Everett, F. Xue, and A. Sabharwal, "Angle-of-arrival based beamforming for FDD massive MIMO," in *Proc. of 49th Asilomar Conference on Signals, Systems and Computers*, 2015, pp. 704–708.

[21] X. Sun, X. Gao, G. Y. Li, and W. Han, "Agglomerative user clustering and downlink group scheduling for FDD massive MIMO systems," in *Proc. of the IEEE International Conference on Communications, (ICC)*, 2017, pp. 1–6.

[22] S. Lloyd, "Least squares quantization in PCM," *IEEE Trans. Inf. Theory*, vol. 28, no. 2, pp. 129–137, 1982.

[23] R. Schmidt, "Multiple emitter location and signal parameter estimation," *IEEE Trans. Antennas Propag.*, vol. 34, no. 3, pp. 276–280, Mar. 1986.

[24] S. Jaeckel, L. Raschkowski, K. Borner, and L. Thiele, "QuaDRiGa: A 3-D multi-cell channel model with time evolution for enabling virtual field trials," *IEEE Trans. Antennas Propag.*, vol. 62, no. 6, pp. 3242–3256, Jun. 2014.

[25] 3GPP, "Study on channel model for frequency spectrum above 6 GHz," 3rd Generation Partnership Project (3GPP), Technical Report (TR) 38.900, Jun. 2017, version 14.3.1.